Electronic Supplementary Information

Synthesis of $Ni_{0.8}Zn_{0.2}Fe_2O_4$-RGO nanocomposite: An excellent magnetically separable catalyst for dye degradation and Microwave absorber

D. Moitra,[a] B. K. Ghosh,[a] M.Chandel,[a] R. K. Jani,[b] M. K. Patra,[b] S. R. Vadera,[b] and N. N. Ghosh,*[a]†

[a]Nano-materials Lab, Department of Chemistry, Birla Institute of Technology and Science, Pilani K.K. Birla Goa Campus, Goa-403726, India.

[b]Defence Lab, Jodhpur 342011, India.

Corresponding author. Tel. /fax: +91 832 2580318/2557033.

E-mail address: naren70@yahoo.com (N. N. Ghosh)

Details of Instrument used to characterize materials

Room temperature powder X-ray diffraction (XRD) pattern of the synthesized nanopowder was recorded using a powder X-Ray diffractometer (Mini Flex II, Rigaku, Japan) with Cu Kα (λ= 0.15405 nm) radiation at a scanning speed of 2°/ min. Thermogravimetric analysis (TGA) analysis were carried out using DTA-60 (Shimaduzu, Japan). Transmission Electron Microscopy (TEM) images of samples were obtained using JEOL JEM 1400, Japan. Fourier transform infrared spectra (FT-IR) were recorded in KBr by using FT-IR spectrophotometer Model Shimadzu DR-8031. Raman spectra were taken on a Renishawin Via Raman microscope with a 633 nm laser excitation. Energy dispersive X-Ray spectra of the synthesized material was recorded using Carl-Zeiss EVOMA15 (Carl-Zeiss, Germany) electron microscope. Room temperature magnetization with respect to external field was measured by using Vibrating Sample Magnetometer (VSM) (EV5, ADE technology, USA).

Details of Experimental procedure for Catalysis Reactions

To study the catalysis reactions Methyl orange (MO, fisher scientific), 4-Nitrophenol (4-NP, Acros organics), Trifluralin (Fluka analytical) and Rhodamine-B (RhB, Fluka analytical) were used Typically 4.5 ml solution of 9 x 10^{-5} (M) 4-NP solution (in case of MO, RhB and trifluralin the concentrations were 6 x 10^{-5}(M), 2 x 10^{-5} (M) and 1.5 x 10^{-5} (M) respectively. Trifluralin solution was prepared in a mixture of alcohol and water) was mixed with 2 ml H_2O and 1 ml 0.2 (N) $NaBH_4$ solutions. To this solution 0.5 ml aqueous suspension of the catalyst (1.25 x 10^{-2} gm/liter) was then added. 3-4 ml of the solution was then immediately transferred into a quartz cuvette. The colored solution faded gradually as the reaction proceeded. The reaction was monitored by recording absorption spectrum by a UV-vis spectrophotometer at an interval of 1 min. After each cycle the catalysts were separated from the reaction mixture by applying external

magnetic field. Then the catalyst were washed several time by deionized water and dried for the next run. All the reaction was carried at room temperature (26 ^{o}C ±1) and the reactions were performed in triplicate. Initially reduction reaction of 4-NP was investigated to obtain the effect type of the catalyst. UV-vis spectra of aqueous solution of 4-NP showed the maximum absorption peak (λ_{max}) at 317nm. This peak was red shifted to 400 nm after addition of $NaBH_4$ due to formation of bright yellow colored 4-nitrophenolate ions.[28, 29] No reaction happened in absence of the catalyst which indicates the catalyst was essential for this reaction. After addition of the catalyst gradually decreases of the peak at 400 nm indicated the progress of the reduction of 4-NP. Also, gradual development of small shoulder peak at 300nm which is attributed to the absorption peak of 4NP was observed.

The catalytic efficiency of 50-NZF-50RGO was also tested towards reduction of MO, RhB and herbicide trifluralin in presence of excess $NaBH_4$. The reaction was monitored spectrophotometrically by following the decrease of absorbance at λ_{max} ($\lambda_{max\ (MO)}$ = 464 nm, $\lambda_{max\ (RhB)}$ = 550 nm, ($\lambda_{max\ (trifluralin)}$ = 439 nm). After separating the catalyst from reaction mixture after reaction, catalyst was washed with alcohol and it was observed that no unreacted dye molecule was remained adsorbed in the catalyst.

Determination of k_{app} of the reactions

It is well documented that, metal oxide nanoparticle catalyzed reduction reaction of dyes and herbicide like trifluralin in presence of excess $NaBH_4$ proceed via pseudo first order kinetics. As the absorbance of the dye is proportional to its concentration, the ratio of absorbance of the dye A_t (measured at time t) to A_o (at t=0) is equal to C_t/C_o (where C_t is the concentration of dye at time t and C_o is the initial concentration of the dye.) The apparent rate constant K_{app} was determined from the following equation:-

$$dC_t/dt = -K_{app}.C_t$$

$$\ln (C_t/C_o) = \ln(A_t/A_o) = - K_{app}.t.$$

The value of k_{app} was calculated from $\ln (A_t/A_o)$ vs. time plot.

Measurement of Microwave absorption of the sample

For the measurement of microwave absorption of the synthesized nanocomposites in X-band (8.2-12.4 GHz range), HP 8510 vector Network Analyzer (USA) was used and reflection loss (RL) was calculated using the measured values of complex permittivity and permeability. To prepare the samples for this purpose, nanocomposites powders were first mixed with aqueous solution of 10 wt % polyvinyl alcohol (PVA) which acted as a binder and the mixture was dried. This mixture was further ground to powders and then compressed under a pressure of 10 tons and shaped into rectangular pellet with size of 10.16 mm x 22.86 mm x 2 mm, so as to fit exactly into rectangular waveguide of X-band.

The reflection loss (RL) was calculated from the complex relative permeability and permittivity at a given frequency and specimen thickness using a model of single-layered plane wave absorber, proposed by Naito and Sutake.[46]

$$Z_{in} = Z_0(\mu_r/\varepsilon_r)^{1/2}\tan h\left[j\left(\frac{2\pi f d}{c}\right)(\mu_r.\varepsilon_r)^{1/2}\right] \qquad \text{(S1)}$$

$$RL = 20\ log\left|\frac{Z_{in} - Z_0}{Z_{in} + Z_0}\right| \qquad \text{(S2)}$$

Where, $\mu_r = \mu' - j\mu''$ and $\varepsilon_r = \varepsilon' - j\varepsilon''$ are the relative complex permeability and permittivity of the absorber medium, respectively, f is the frequency of the electromagnetic wave, d is the absorber

thickness, c is the velocity of light, Z_0 is the free space impedance, and Z_{in} is the absorber impedance. In order to analyse the variation of microwave absorption properties with thickness of the absorber, the reflection loss was calculated using equations (S1) and (S2) for different absorber thickness.

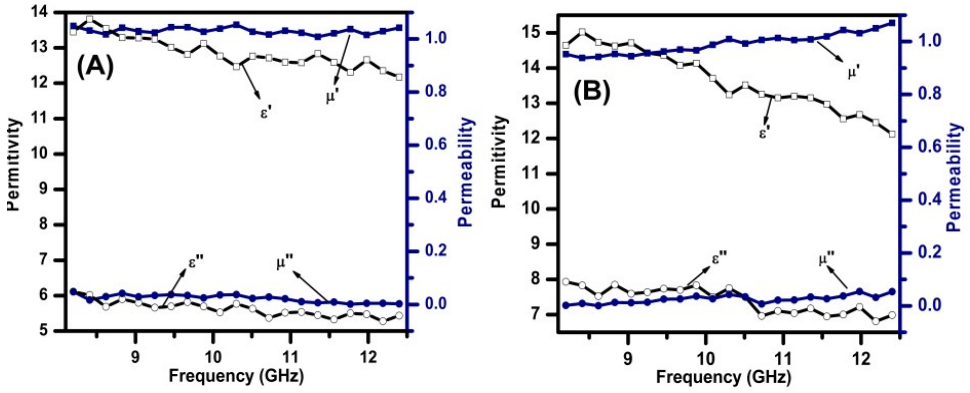

Fig. S1 Frequency dependent permittivity and permeability of (A) pure NZF and (B) 50NZF-50RGO nanocomposite.

Synthesis of Materials

Materials Used

Nickel nitrate $Ni(NO_3)_2.6H_2O$, Zinc nitrate $Zn(NO_3)_2.6H_2O$, Iron nitrate $Fe(NO_3)_3.9H_2O$, Sodium hydroxide (NaOH), Sodium nitrate $NaNO_3$, Sulphuric acid (H_2SO_4), Potassium permanganate ($KMnO_4$) and 30% H_2O_2 solution were purchased from Merck, India and Graphite powder (bought from Sigma Aldrich with mean particle size of < 20 μm) and used without further purification. Deionized water was used throughout the experiment.

Synthesis of Graphene Oxide

Graphene Oxide was synthesized from Graphite powder according to method reported by Hummers and Offeman.[47] In this synthesis process, at first 1 g graphite and 0.6 g of $NaNO_3$ were mixed with 35 ml of H_2SO_4 (18M) at 0°C. The mixture was stirred for 6 h. Then 3.8 g of $KMnO_4$

was added to the suspension very slowly. The temperature of the solution rises to 35°C and was maintained for 8 h so that complete oxidation takes place. Then 60 ml of distilled H_2O was slowly added and the reaction temperature was increased to 98°C. This temperature was maintained for 1 h and finally 2 ml of 30 % H_2O_2 solution was added into the mixture and stirred for 0.5 h. The mixture was centrifuged and washed with 10 % HCl solution and distilled H_2O. The yellowish brown precipitate of graphene oxide was obtained and dried at 60°C.

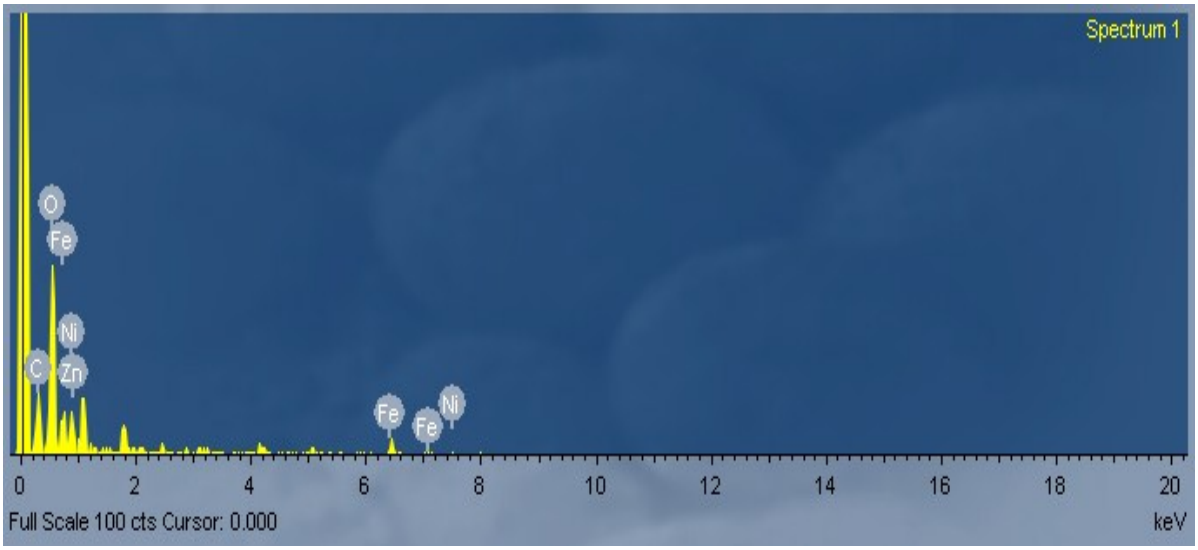

Fig. S2 EDAX spectra of synthesized 50NZF-50RGO nanocomposite.

Thermal analysis of NZF-RGO composite

TGA analysis of GO and NZF-RGO was performed in air atmosphere in the temperature range of 30-850°C with heat rate 10°C /min. Fig. S3 shows TGA thermograms of pure GO and NZF-RGO nanocomposites having various compositions. In TGA thermograms following points were observed (i) in the temperature of 30-100°C, GO showed ~17% wt. loss, which might be due to evaporation of H_2O.[11] In this temperature range ~9% wt. loss occurred for 50NZF-50RGO. (ii) In 100-200°C temperature range, GO showed ~3% wt. loss and a sharp weight loss occurred in the range of 200-250°C with 15% weight loss. This was due to the removal of oxygen containing groups from GO. However, only 9% wt. loss occurred for 50NZF-50RGO. This fact clearly indicated that during synthesis of NZF-RGO, GO was converted to RGO via reduction of oxygen containing groups (e.g. carbonyl, carboxyl, epoxy groups, etc.) [11] during reflux with NaOH. (iii) In 325-600°C temperature range, the oxidative decomposition of carbon atoms of GO was observed whereas, in case of 50NZF-50RGO, this decomposition of carbon occurred in the range of 275-375°C. It was also observed that, ~50wt% NZF remained undecomposed as residue. Similarly for 85NZF-15RGO, 75NZF-25RGO and 50NZF-50RGO nanocomposites 85wt%, 75wt% and 50wt% NZF was remained as residue after thermal decomposition of the RGO component of the composites. So, we can also conclude that, this 'in situ co-precipitation' method for NZF-RGO composite preparation is capable of producing composites with desired NZF and RGO composition.

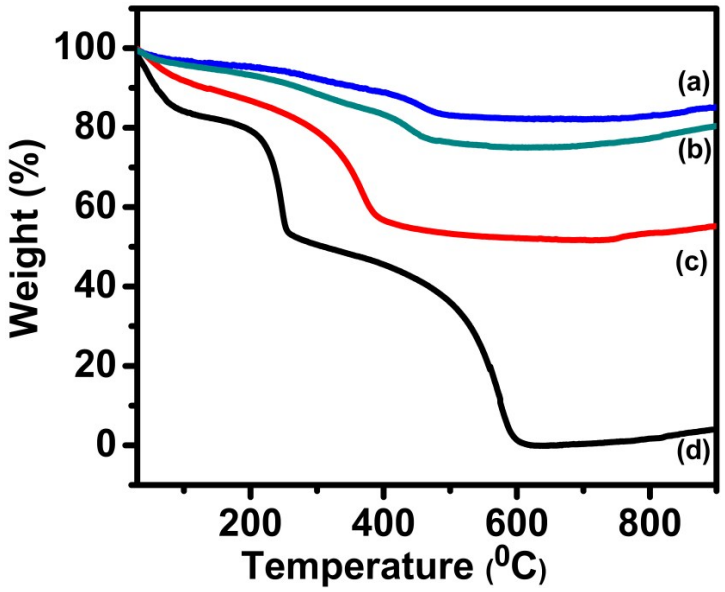

Fig. S3 TGA curves of (a) 85NZF-15RGO (b) 75NZF-25RGO (c) 50NZF-50RGO nanocomposite and (d) GO.

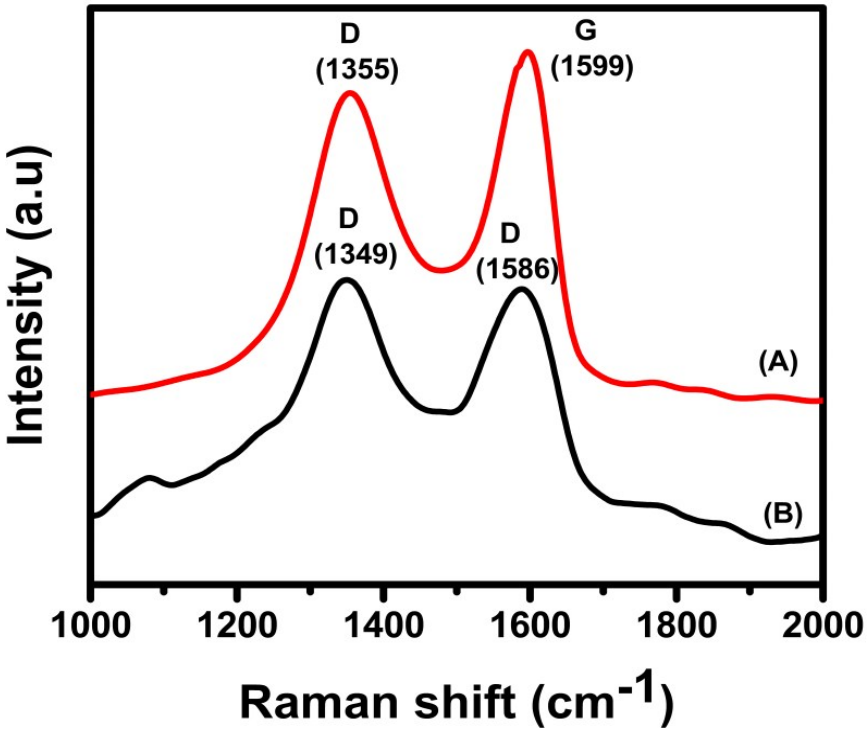

Fig. S4 Raman spectra of (A) GO and (B) 50NZF -50RGO.

The apparent rate constant for reduction of various dyes and the completion times are listed in Table S1.

Table S1: Completion time and rate constants of 50NZF-50RGO catalyzed reduction reactions.

Dyes	Completion Time (min)	Rate Constant (k_{app}) (min^{-1})	Correlation Coefficient
4-NP	6 (±0.14)	0.73 (± 0.03)	0.96
MO	5 (±0.25)	0.95 (± 0.05)	0.96
RhB	7 (±0.14)	0.71 (± 0.02)	0.97
Trifluralin	20 (±0.5)	0.15 (± 0.01)	0.99

Times required for completion of reduction reactions are given in Table S2. These data clearly showed that least time was required when catalysis reaction was performed using 50NZF-50RGO as catalyst and the catalytic efficiency of NZF-RGO catalysts was found to be decreased when RGO component in the catalyst was more than 50 wt. %.

Table S2 Times required to complete the reduction reaction of various dyes catalyzed by NZF-RGO composites.

Catalyst composition	Time required to complete the reaction		
	4-NP	MO	RhB
NZF	15 min	17 min	19 min
85NZF-15RGO	12 min	15 min	16 min
75NZF-25RGO	9 min	11 min	12 min
50NZF-50RGO	6 min	5 min	7 min
25NZF-75RGO	14 min	14 min	18 min

Catalytic activity of NZF-RGO nano composites towards degradation of 4-NP, RhB and MO in presence of excess $NaBH_4$

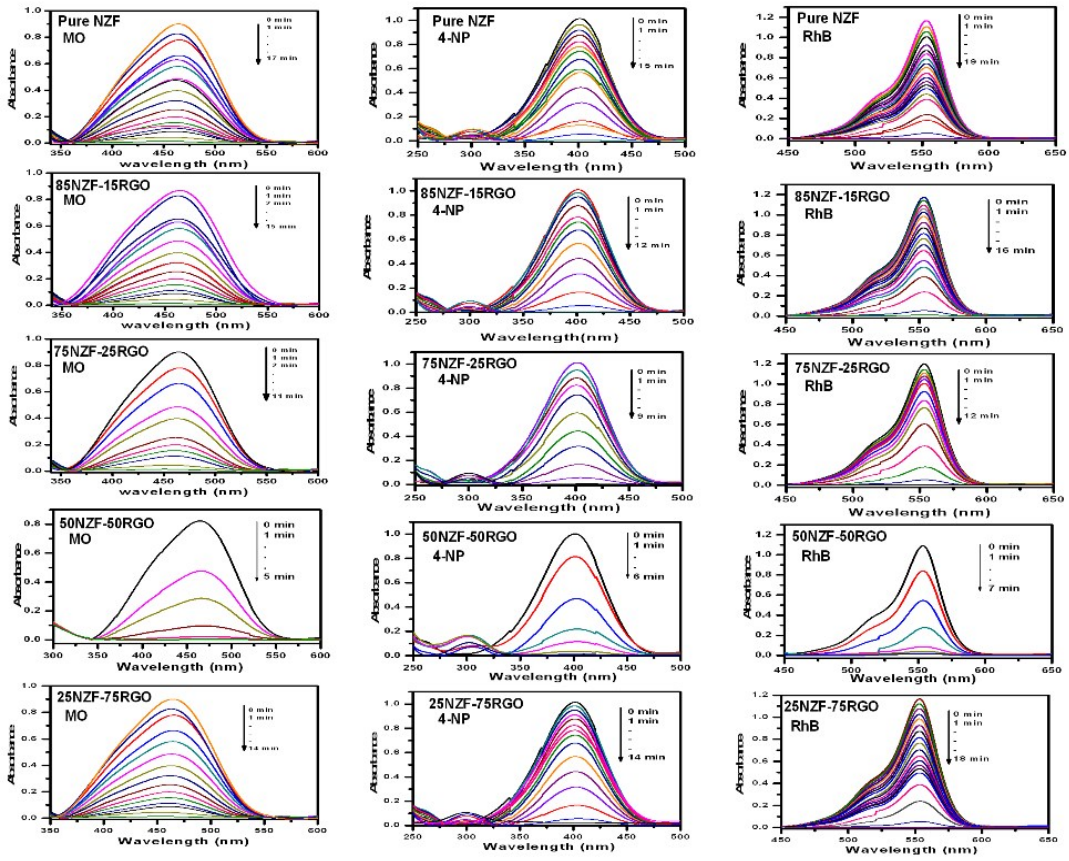

Fig. S5 Time dependent spectral changes of the reduction reactions of various dyes catalyzed by NZF-RGO nanocomposites, having various compositions.

Reusability study of 50NZF-50RGO catalyst.

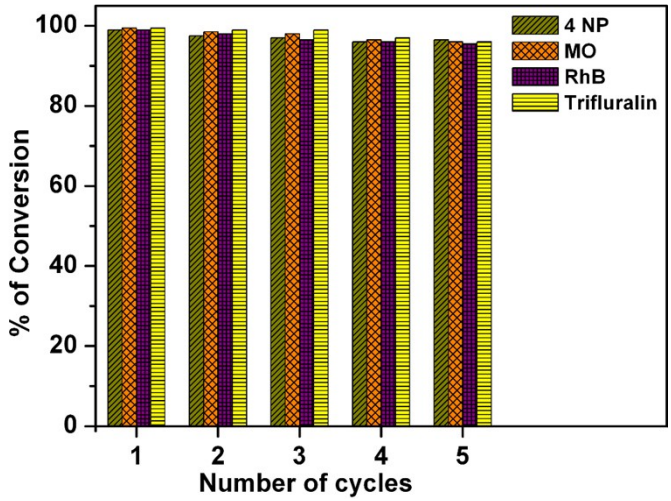

Fig. S6 Reusability of magnetically separable catalyst (50NZF-50RGO) for the reduction of 4-NP, MO, RhB and Trifluralin.

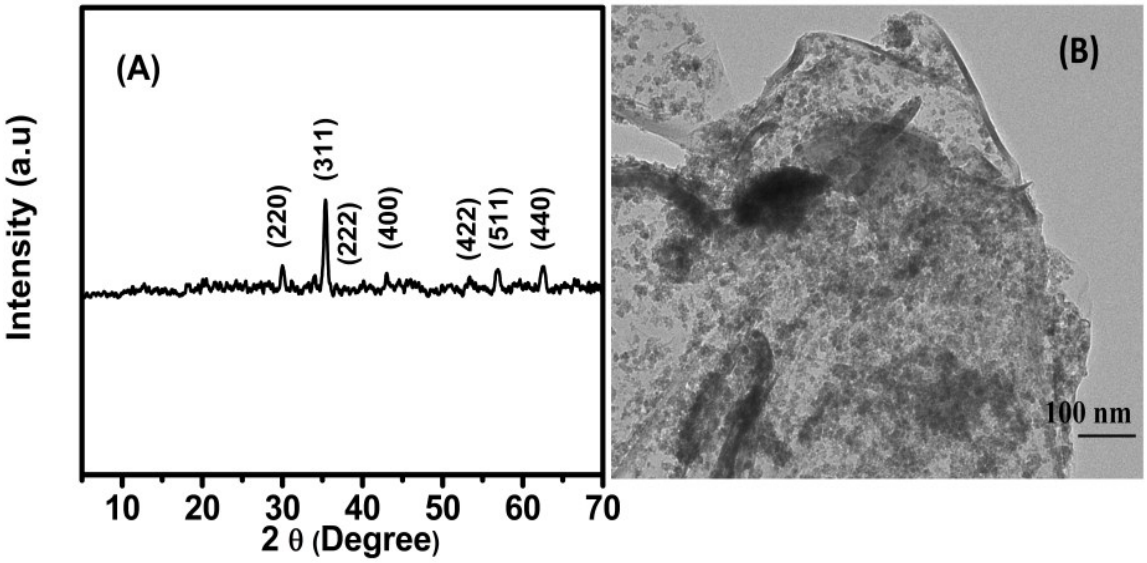

Fig. S7 (A) XRD and (B) TEM micrograph of the recycled catalyst 50NZF – 50RGO.

Magnetic property of NZF-RGO nanocomposite

Room temperature magnetic property measurement of synthesized NZF and NZF-RGO nanopowders were measured by vibrating sample magnetometer (VSM) as shown in Fig. 5. The values of magnetic parameter corresponding to Fig. 5 are shown in Table S3.

Table S3: Magnetic properties of NZF and NZF-RGO nanocomposites

Sample	M_s (emu.g^{-1})	H_c (Oe)
Pure NZF	42	7.674
85NZF-15RGO	34	4.101
75NZF-25RGO	25	2.389
50NZF-50RGO	14	0.361

It is clear from Table-S3 that with increasing graphene content in the NZF-RGO composites the values of saturation magnetization (M_s) and coercivity (H_c) were decreased. The low coercivity value, of NZF and NZF-RGO composites showed typical super paramagnetic behavior

Table S4: Microwave absorption of GO, RGO and synthesized 50NZF-50RGO nanocomposite

GO	-28.5 dB	5 mm	2.6 GHz	71
RGO	-10 dB	-	16 GHz	72
RGO	-7 dB	2 mm	6.5 GHz	73
RGO	-6.11 dB	2 mm	6.1 GHz	74
RGO	-8.0 dB	4 mm	2.4 GHz	75
NZF	-13.61 dB	1.9 mm	10.72 GHz	Present work
50NZF-50RGO	-19.99 dB	1.8 mm	11.58 GHz	Present work

71. P. M. Sudeep, S. Vinayasree, P. Mohanan, P. M.Ajayan, T. N. Narayanan and M. R. Anantharaman, *Appl. Phys. Lett.*, 2015, **106**, 221603.

72. E. Ma, J. Li, N. Zhao, E. Liu, C. He and C. Shi, *Mater. Lett.*, 2013, **91**, 209.

73. C. Wang, X. Han, P. Xu, X. zang, Y. Du, S. Hu, J. Wang and X. Wang, *Appl. Phys. Lett.*, 2011, **98**, 072906.

74. X. Wang, M. Yu, W. Zang, B. Zang and L. Dong, *Appl. Phys. A*., 2015, **118**, 1053.

75. X. Sun, J. He, G. Li, J. Tang, T. Wang, Y. Guo and H. Xue, *J. Mater. Chem. C.*, 2013, **1**, 765.

Table. S 5: Microwave absorption properties of various ferrites and ferrite composites

Sample	Preparation method	Minimum RL	Corresponding frequency	Absorber thickness	Effective band width (RL< -10dB)	Reference
Ni Zn ferrite	Calcined at 1200˚C for 2h	-16 dB	10.6 GHz	2 mm		78
$Ni_{0.3}Zn_{0.5}Fe_2O_4$/PEG	Hydrothermal followed 200˚C	-50.15 dB	a) 8.8 GHz	2.9 mm		79
$NiFe_2O_4$(65 wt%)/polystyrene	Calcined at 800˚C for 2h	-13 dB	11.5GHz	2 mm.	10.3–13GHz (2.7 GHz)	80
$(Ni_{0.4}Co_{0.2}Zn_{0.4})Fe_2O_4$	Sintered at 1250˚C for 2h.	−17.01 dB	6.1GHz	3 mm		81
Ag core shell $Ni_{0.5}Zn_{0.5}Fe_2O_4$	Hydrothermal at 180˚C for 3h.	-25 dB	9.0 GHz	1-2 mm		22
$ZnFe_2O_4$/RGO	Hydrothermal synthesis at 180˚C	-29.3 dB	16.7 GHz	1.6 mm	2.6 GHz (15.4-18 GHz)	36
$ZnFe_2O_4$/ppy	80˚C for 8h	-28.9 dB	10.8 GHz	2.7 mm		82
$CoFe_2O_4$ hollow / Graphene composites	Vapour diffusion followed by calcination at 550˚C	-18.5 dB	12.9 GHz	2 mm	3.7 GHz.	40
a) EG/PANI/ CoFe2O4 with m_{CF}/ m_{EG}/ $m_{PANi}$of 0.8 b) CoFe2O4	Co-precipitation method and sintered at 300˚C	a) -19.13 dB b)-13.58 dB	a)13.28 GHz b) 14.83 GHz	a) 0.5 mm b) 1 mm	a) 5.94GHz. b)3.6 GHz.	83
CNT/ $CoFe_2O_4$	Chemical Vapor Deposition	a) -18 dB	a) 9 GHz			84
Hollow glass microsphere/$CoFe_2O_4$	Co-precipitation method	a)-8.3 dB	a)18 GHz	a) 1.5 mm		85
$CoFe_2O_4$ nanorod/Graphene	Hydrothermal at 150˚C	a) -25.8 dB	a) 16.1 GHz	a) 2.0 mm	4.5 GHz was.	86

Rugby Shaped $CoFe_2O_4$	Vapour diffusion followed by calcination at 550˚C	a) -34.1 dB	a) 13.4 GHz	a) 2.5 mm	2.6 GHz.	87
$CoFe_2O_4$/ SBA-15	double solvent technique and impregnation method	-18 dB	16 GHz	2 mm	4.5 GHz.	88
Polyaniline - $CoFe_2O_4$	Calcined at 1000˚C followed by situ emulsion polymerization	-21.5dB				89
$Ni_{0.5}Co_{0.5}Fe_2O_4$	coprecipitation	-18 dB	2.5 GHz	1.5 mm		23
Graphene– Fe_3O_4 hybrid spheres	Heated at 200^{o}C for 24h,	-20 dB	16 GHz	5mm		90
RGO/$CoFe_2O_4$ composite	One-pot hydrothermal route at180^{o}C for10h	-47.9dB	12.4 GHz	2.3 mm		11
30 wt.% hollow Fe_3O_4/RGO	Solvothermal method. 200^{o}C for 12h.	-24 dB	12.9 GHz	2.0 mm	4.9 GHz	39
N-RGO–hematite–wax composites loading of 15 wt%.	reflux at 80^{o}C for 2 h.	-90.2 dB	6.1 GHz	4.5 mm		56
NZF	coprecipitation method at 120^{o}C for 12h	-13.61 dB	10.72 GHz	1.9 mm	9.8-12 GHz	Present work
50NZF-50RGO nanocomposite	In situ coprecipitation method at 120^{o}C for 12h	-19.99 dB	11.58 GHz	1.8 mm	10.22- 12.4 GHz	This work

References

78. A. Miszezyk and K. Darowicki, *Anti. Corros. Method. M.,* 2011, **58**, 13.

79. Q. Li, Y. Li, X. Li, S. Chen, S. Zang, J. Wang and C. Hou, *J. Alloys Compd.*, 2014, **608**,

80. H. Zhao, X. Sun, C. Mao and J. Du, *Physica B*, 2009, **404**, 69.

81. D. L. Zhao, Q. Lv and Z. M. Shen, *J. Alloy. Compd.*, 2009, **480**, 634.

22. C. H. Peng, H. W. Wang, S. W. Kan, M. Z. Shen, Y. M. Wei and S. Y. Chen, *J. Magn. Magn. Mater.*, 2004, 284, 113.

36. Z. Yang, Y. Wan, G. Xiong, D. Li, Q. Li, C. Ma, R. Guo and H. Luo, *Mater. Res. Bull.*, 2015, **61**, 292.

82. Y. Li, R. Yi, A. Yan, L. Deng, K. Zhou, X. Liu, *Solid State Sci.*, 2009, **11**, 1319.

40. M. Fu, Q. Jiao, Y. Zhao and H. Li, *J. Mater. Chem. A.*, 2014, 2, 735.

83. K. Chen, C. Xiang, L. Li, H. Qian, Q. Xiao and F. Xu, *J. Mater. Chem*., 2012, **22**, 6449.

84. R. C. Che, C. Y. Zhi, C. Y. Liang and X. G. Zhou, *Appl. Phys. Lett.*, 2006, **88**, 033105.

85. W. Fu, S. Liu, W. Fan, H. Yang, X. Pang, J. Xu and G. Zou, *J. Magn. Magn. Mater.*, 2007, **316**, 54.

86. M. Fu, Q. Jiao and Y. Zhao, *Mater. Charact.*, 2013, **86**, 303.

87. S. Zhang, Q. Jiao, Y. Zhao, H. Li and Q. Wu, *J. Mater. Chem. A*., 2014, **2**, 18033.

88. L. G. Min, W. L. Cheng, and X. Yao, *Chin. Phys. B.*, 2014, **23**, 088105.

89. N. Gandhi, K. Singh, A. Ohlan, D.P. Singh and S.K. Dhawan, *Compos. Sci. Technol.*, 2011, **71**, 1754.

23. K. Khan, *J. Supercond. Novel Magn.,* 2014, **27**, 453.

90. W. Xue, R. Zhao, X. Du, F. Xu, M. Xu and K. Wei, *Mater. Res. Bull.,* 2014, **50**, 285.

11. M. Zong, Y. Huang, Y. Zhao, X. Sun, C. Qu, D. Luo and J. Zheng, *RSC Adv*., 2013, **3**, 23638.

39. H. L. Xu, H. Bi, and R. B. Yang, *J. Appl. Phys.,* 2012, **111**, 07A522.

56. D. Chen, G.-S. Wang, S. He, J. Liu, L. Guo and M. S. Cao, *J. Mater. Chem. A*., 2013, 1, 5996-6003.